International Symposium of Research Students on Material Science and Engineering
December 20-22, 2004, Chennai, India
Department of Metallurgical and Materials Engineering, Indian Institute of Technology Madras

INTERFACE MEDIATED GROWTH OF THIN PENTACENE FILMS

A. Al-Mahboob, J. T. Sadowski, Y. Fujikawa, T. Nagao, K. Nakajima and T. Kurai

Institute for Materials Research, Tohoku University, 2-1-1 Katahira, Aoba-ku, Sendai 980-8577, Japan

ABSTRACT

Annealed, well ordered Bi(001)/Si(111) films have been used as the substrates for the growth of pentacene (Pn). We determined using low energy electron microscopy (LEEM) and scanning tunneling microscopy (STM) that the pentacene molecules "stand up" on the Bi(001) surface, growing in a bulk-like structure directly from first layer, and that they are very well-ordered. Sharp low energy electron diffraction (LEED) patterns and STM observation of the one-dimensional Moiré fringes indicate that the Pn layer is aligned with the Bi(001) substrate having "point-on-line" commensurate relation along <100> directions. By analyzing the contrast modulation in the STM images we determined the commensurate epitaxial relation between Pn film and Bi(001) substrates.

Keywords: LEEM, STM, pentacene, thin film, vacuum deposition

1. INTRODUCTION

The microelectronics industry has long concentrated on inorganic materials, such as silicon and gallium arsenide, but recent progress in the field of organic thin-film transistors (OTFTs)[1-7] receives significant attention. Practical applications of such devices require inexpensive organic films deposited on a variety of substrates. Pentacene ($C_{22}H_{14}$) was found to be particularly promising, since it has been successfully used in OTFTs with field-effect mobilities matching[7] or even surpassing[2] that of amorphous silicon. Pentacene (Pn) can be relatively easily grown on wide range of substrates, from insulators[3-4,8] and semiconductors[9] to metals[8,10-11]. The fabrication of the pentacene FET transistors on plastic substrates has been also demonstrated[1], which makes Pn a promising material for constructing low-cost, large area electronic and optoelectronic devices, flexible displays, etc.

In most of the cases mentioned above, flat laying first layer (metal substrates) or wetting layer[8-10,12] (often disordered) is formed before ordered, 'standing up' molecular structure eventually appears. It is well established that the electrical conduction in OTFT is strongly affected by defects and the structure of the interface[13]. Since the anisotropy of the carrier mobility is very high in π-conjugated organic semiconductors like Pn[14], it is very important to understand the fundamental mechanisms that control both, the morphology and the electronic structure at the interface between metal and organic materials. In case of pentacene, the balance between two interactions: a weak, Van der Waals – type Pn-Pn interaction and the interaction between pentacene molecule and the substrate is responsible for the orientation of the Pn film. Results of the recent experiments show that the latter interaction strongly depends on the substrate surface electronic structure[8,15]. We have found that thin, well ordered film of semimetal bismuth is interesting candidate for the use as a substrate in the growth of organic films, having the electronic structure intermediate between metallic and insulating substrates used for pentacene

growth up to date. We found that the pentacene grows epitaxially on Bi(001) at room temperature having 'standing up' structure from the first layer. Since recent angle-resolved photoemission spectroscopy (ARPES) experiments on the bulk-terminated Bi(001) surface showed the existence of pseudo-gaps formed from bands confined to the topmost bilayer that are within 1 eV below the Fermi level[16], we expect only a weak interaction between the insulating Bi(001) surface and Pn molecules.

2. EXPERIMENTAL SETUP

Pentacene has been thermally evaporated in-situ in two separate ultra-high vacuum (UHV) systems: low energy electron microscope (LEEM) and scanning tunneling microscope (STM), respectively. The Bi(001)/Si(111) films with thickness of ~30 BL, annealed in-situ at ~400K to improve their morphology[17], were used as the substrates for Pn growth. Pn was deposited at RT from the tantalum crucible. The deposition rate was in the range of 0.02 ÷ 0.1 ML/min, where 1 ML corresponds to the molecular density of the Pn(001) plane. Growth of Pn was observed in real time in LEEM, with imaging electron energy as low as 0.2 eV in order to avoid desorption of the Pn film caused by electron irradiation. LEED diffraction patterns were recorded in the LEEM[18] experiment with electron energy of ~16 eV, and they were taken simultaneously from the clean Bi(001) surface, as well as Bi(001) surface partially or completely covered by the first Pn layer. In a separate experiment, the STM images were taken from the approximately 1 ML thick Pn film deposited at room temperature onto Bi(001).

3. RESULTS AND DISCUSSION

Bulk crystal structure of bismuth is rhomboedral[19] with 2 atoms per unit cell, which can be also understood as pseudo-cubic[19-20]. Cleaving along (111) creates the surface of hexagonal symmetry with no chemical bonds normal to the surface[19], resulting in the intra-bilayer covalent bonds and inter-bilayer metallic or Van der Waals bonds, as shown in Fig.1. The (111) plane of rhombohedral Bi is called in this paper the (001) for crystal indexing, or simply (00) for surface indexing, with the simplest hexagonal coordinates, $|a| = |b| = 4.546$ Å and trigonal axis $|c| = 11.862$ Å. Here, a bilayer (BL_{001}) is the smallest unit in the [001] direction, with BL step height of 3.9 Å. The (00) plane in our surface indexing and (001) plane in crystal indexing correspond to the (111) plane of both, rhomboedral Bi and cubic substrate Si, respectively. In the recent work[21] it has been determined that during the UHV Bi deposition on Si(111)-7x7 at room temperature, the film undergoes an unique and unexpected structural phase transformation from the pseudocubic {012} phase into a hexagonal Bi(001) phase – the same as bulk terminated Bi. The morphology of the Bi(001) film can be further improved by moderate annealing[17], as shown in Fig.2. Fig.2a is the topographic STM image of the as deposited Bi(001) on Si(111), showing triangular islands of hexagonal symmetry, while Fig.2b is the is the topographic STM image of the same region after annealing at ~410K, showing wide terraces aligned along Si steps laying underneath. The high resolution STM image taken from the terrace of Fig.2b is shown in Fig.3c. It reveals the same hexagonal symmetry of bulk terminated Bi(001) having no chemical bonds normal to the surface, as sketched in Fig.1.

Flat and well ordered, annealed Bi films have been subsequently used as the substrates for the pentacene growth. Pentacene is a flat, elongated molecule, consisting of five π-conjugated, aromatic, benzene-like rings fused sideways along long molecular axis (LMA). Its bulk phase has a triclinic crystal structure[22-23] with 2 molecules per unit cell and it forms a layered structure with the herringbone arrangement in the direction of the short molecular axis (SMA) parallel to the (001) plane (called also ab plane). Northrup et al. showed by the first-principles pseudopotential density-functional calculations[24] that the (001) plane has much lower surface energy than other low index planes and the steps along short axis (a-axis) have the lowest step

energy. The bonds between molecules in the same layer (ab plane) are several times stronger than those between molecules in adjacent layers. This anisotropy in the bonding is a driving force for the film to exhibit self-organized (001) – "standing up" orientation, when deposited on a substrate with which Pn interacts weakly.

From LEEM observation of Pn growth in the real time[25], we found that Pn molecules are highly mobile on Bi(001) surface. Very low nucleation density and the high mobility of Pn molecules on the Bi(001) surface result in the sizes of the first-layer Pn islands exceeding ~0.2 mm, which is among the largest reported to date. During the formation of the first Pn layer, some triangular holes are remaining initially uncovered. They are gradually filling up due to additional deposition and the diffusion of ad-molecules from the terrace of Pn where no nucleation of the second layer has occurred yet. The growth mode of first Pn layer appears to be a step-flow growth, as shown in the Fig.3a. At the growth front, the parallel step segments move rapidly and step segments of triangular slopes in relation to the average step direction grow slowly, leaving initially some holes in the first Pn layer. We anticipate that this is due to the step energy anisotropy of the Pn and the pinning of the ad-molecules at Bi steps (or Bi grain boundaries).

LEED diffraction pattern taken from the Bi(001) surface partially covered by the first Pn layer (Fig.3a) is shown in Fig.3b. Spots originating only from the Bi(001) surface are marked with solid circles while those coming from the overlapping Bi and Pn patterns are marked by broken circles. Pn (02) diffraction spot exactly overlaps with Bi(01) spot of the annealed Bi(001) film that is relaxed to the bulk-like structure, which means that <10> directions of both Bi and Pn are identical. The Pn unit cell short diagonal, <-11> (the corresponding diffraction spot (11)), and long diagonal, <11> (the corresponding diffraction spot (1-1)) are angled anti-clockwise and clockwise with crystal directions <01> (the corresponding diffraction spot (10)), and <11> (the corresponding diffraction spot (1-1)) of Bi respectively. Here, '< >' stands for the crystal direction of surface lattices. The in-plane unit cell parameters for the Pn(001) plane (ab plane), obtained from the analysis of the LEED diffraction patterns are:

$$|a_{LEED}| = 6.1 \pm 0.2 \text{ Å}, |b_{LEED}| = 7.893 \pm 0.005 \text{Å} \quad \text{and } \gamma_{LEED} = 86^{o} \pm 0.5^{o} \qquad (1)$$

Basing on the LEED diffraction pattern, we propose a model for the 'point-on-line' commensurate adsorption geometry of the first Pn layer on Bi(001)[25], as shown in Fig.3c. Shorter axis of Pn lattice (a-axis) is aligned along the [10] direction of Bi-hexagonal surface. The distance between equivalent (01) Pn molecular arrays – interplane distance of Pn(010) planes in the direction perpendicular to surface normal – is in the following relation with Bi lattice:

$$d(|b_{Pn}|) = \sqrt{3}|a_{Bi}| \qquad (2)$$

where $|a_{Bi}| = 4.546$ Å is the inter-atomic distance in the Bi(001) plane.

The exact epitaxial relations are subsequently determined from the STM contrast modulation, since the 'point-on-line' commensurate relation can also be revealed by observing the periodic one-dimensional Moiré fringes[26] in STM images, originating from the overlapping of the oblique surface lattice of Pn with the hexagonal Bi lattice at interface. The exact epitaxial relation can be analyzed via lattice transformation relations between parent and product in relation to equivalent lattices positions at the interface[27].

The empty state, high-resolution STM image shown in Fig.4a is recorded on the first Pn layer and it shows rows of brighter and darker protrusions. Each protrusion corresponds to a single Pn molecule. The Pn unit cell viewed along the axis normal to Bi(001) substrate is outlined in the STM image. The contrast difference between molecules is consistent with the fact that the two

molecules in the unit cell are inequivalent, having herringbone arrangement in the Pn(001) plane. In order to understand the origin of this contrast difference, we simulated the Mulliken[28] charges and bond population in identical and non-identical Pn molecules perturbed only by Pn-Pn interaction in a single isolated monolayer, unperturbed by interface, in density functional theory (DFT) with generalized gradient approximation (GGA) using pseudo-potential and RPBE[29] functionals. DFT analysis shows that Pn having SMA oriented with small angle along long diagonal of surface unit cell is more electronegative (by an amount of 0.1 electronic charge) than non-identical Pn having SMA oriented with small angle along short diagonal. It is possible that the net charge transfer between two molecules results in a different contrast in STM images of identical and non-identical Pn molecules.

Constant height, empty state STM image of 1ML Pn on Bi (001), Fig.4b, shows additional contrast modulation induced by the interface – even some originally darker molecules in certain unit cells are brighter than these in other unit cells. The same feature is reproduced at every lattice translation by supercell lattice vectors given by the relation:

$$a_0=4a_{Pn}-4b_{Pn}, \quad b_0=4a_{Pn}+5b_{Pn} \tag{3}$$

and by any integral combination of a_0 and b_0. It may be expected here that this contrast modulation arises from the charge transfer or interference of electronic states at interface. It will be sufficient for analyzing the epitaxial relations, if we consider that the contrast modulation observed in the STM images is a function of relative positions of Pn molecules with respect to Bi atoms at interface. We assume therefore that the repetition of modulated features is the same as repetition of equivalently correlated position, satisfying the lattice translations in both hexagonal Bi and oblique Pn lattices. As the 'point-on-line' commensurate structure is observed in LEED patterns, we expect to observe the one-dimensional periodic Moiré fringes in the constant height STM images. Fig.4c shows an example of the one-dimensional periodic Moiré fringes observed in STM. For better visualization, we filtered out most of the periodic features except the Moiré modulation, using the fast Fourier transformation (FFT) filter[30]. From the analysis of the contrast modulation and solving the equations for the supercell lattice vectors a_0 and b_0 (by lattice transformations in the both Pn surface lattice (ab plane) and hexagonal Bi lattice, considering equation (1) and 'point on line' commensurate relation determined from LEED), we determined precisely the epitaxial relations and lattice parameters of ab Pn plane. According to these, the direction of Moiré fringe, the lattice translation:

$$T= b_0-2a_0=13b-4a \tag{4}$$

is aligned at an angle $\gamma_0= 100.07^o$ with the Pn a-axis, and the fringes have the perpendicular periodicity of 16.87Å. The epitaxial relations are as follows:

$$a_{Pn}=49/36a_{Bi},\ b_{Pn}=10/9a_{Bi}+2b_{Bi},\ \gamma=\text{arc cot}(1/9\sqrt{3}) \tag{5}$$
$$|a_{Pn}|=6.188\text{Å},\ |b_{Pn}|=\sqrt{3}|a_{Bi}|/\sin\gamma=7.891 \text{ and } \gamma=86.330^\circ$$
$$a_0=4a_{Pn}-4b_{Pn}=a_{Bi}-8b_{Bi}, \quad b_0=4a_{Pn}+5b_{Pn} = 11a_{Bi}+10b_{Bi}$$

Here subscripts 'Pn', 'Bi' and '0' denote the Pn surface (ab-plane) lattice, Bi hexagonal lattice and supercell lattice parameters, respectively. The above vector relations imply that supercell is 36 times larger than the Pn unit cell. Closest two, non-collinear, equivalent Pn molecular positions with respect to an arbitrary origin, i.e. lattice vectors in equivalent lattice a_0 and b_0, have the magnitudes of $\sqrt{73}|a_{Bi}|$ and $\sqrt{111}|a_{Bi}|$, and angles with Pn a-axis of -54.18° and 55.29°, respectively. Simulated, superimposed geometry of oblique Pn and hexagonal Bi lattices at interface, shows periodic one dimensional Moiré fringes of the same periodicity and directions as observed in STM, in agreement with analyzed epitaxial relations (Fig.4c).

4. CONCLUSIONS

It is evident from both, STM and LEEM study, that the 'point-on-line' commensurate relation along a-axis exists, however it has been noted that supercell is 36 times larger than the unit cell of adsorbed molecular species. Step formation energy is lowest along the short axis[24] of Pn, and spacing of alternate adsorbed molecular arrays in this direction is matching exactly with that of substrates, and therefore the 'point-on-line' commensurate relation is helping to maintain the high ordering of Pn film in this direction. Regarding the very low nucleation density, the nucleation may favorably occur at the step edge or grain boundary parallel to a hexagonal axis, where some Bi bonds are cut and/or possibly have different electronic character and metallicity[31]. No epitaxial matching along hexagonal axes other than that along a-axis of Pn has been observed, thus the growth front of the Pn film is not altered by the presence of the hexagonal grain boundaries on Bi(001) surface. Pinning of ad-molecules at the steps or grain boundaries other than a-axis is less favorable. Moreover, the attachments of ad-molecules along a-axis are energetically favorable also due to the lowest step energy for the steps parallel a-axis. As the result, the existence of 'point on-line commensurate' relation along the steps having the lowest step energy and the existence of only one Bi crystallographic axis of epitaxial matching along that step direction (the a-axis of Pn), provide highly ordered, large area, single crystal of Pn. Highly ordered single crystalline first layer, as grown in our experiments, will provide better crystallinity of Pn due to reduced number of interfacial defects. This is confirmed from high crystallinity of thick film deposited on Bi(001) which is derived from the photoluminescence data[31] and presently under further investigations.

REFERENCES

1. C. D. Dimitrakopoulos, S. Purushothaman, J. Kymissis, A. Callegari, J. M. Shaw, Science 283 (1999) 822.
2. C. D. Dimitrakopoulos, J. Kymissis, S. Purushothaman, D. A. Neumayer, P. R. Duncombe, R. B. Laibowitz, Adv. Mater. 11 (1999) 1372.
3. C. D. Dimitrakopoulos, A. R. Brown, A. Pomp, J. Appl. Phys. 80 (1996) 2501.
4. A. R. Brown, A. Pomp, C. M. Hart, and D. M. de Leeuw, Science 270 (1995) 972.
5. A. Dodabalapur, Z. Bao, A. Makhija, J.G. Laquindanum, V.R. Raju, Y. Feng, H.E. Katz, J. Rogers, Appl. Phys. Lett. 73 (1998) 142.
6. H. Sirringhaus, N. Tessler, R.H. Friend, Science 280 (1998) 1741.
7. S.F. Nelson, Y.Y. Lin, D.J. Gundlach, T.N. Jackson, Appl. Phys. Lett. 72 (1998) 1854.
8. P. G. Schroeder, C. B. France, J. B. Park, B. A. Parkinson, J. Appl. Phys. 91 (2002) 3010.
9. F. - J. Meyer zu Heringdorf, M. C. Reuter, R. M. Tromp, Nature 412 (2001) 517.
10. L. Casalis, M. F. Danisman, B. Nickel, B. Bracco, T. Toccoli, S. Ianotta, G. Scoles, Phys. Rev. Lett. 90 (2003) 206101.
11. Q. Chen, A. J. McDowall, N. V. Richardson, Langmuir 19 (2003) 10164.
12. Robert J. Hamers, Nature 412 (2001) 489.
13. M. Pope and C. E. Swenberg, Electronic Processes in Organic Crystals and Polymers, 2nd ed., Oxford University Press, New York (1999).
14. Oana D. Jurchescu, Jacob Baas, and Thomas T. M. Palstra, Appl. Phys. Lett. 84 (2004) 3061.
15. G. E. Thayer et al., manuscript in preparation.
16. C. R. Ast and H. Höchst, Phys. Rev. B67 (2003) 113102.
17. S. Yaginuma, T. Nagao, J. T. Sadowski, A. Pucci, Y. Fujikawa, T. Sakurai, Surf. Sci. 547 (2003) L877.
18. E. Bauer, Rep. Prog. Phys. 57 (1994) 895.
19. F. Jona, Surf. Sci. 8 (1967) 57.
20. G. Jezequel, J. Thomas and I. Pollini, Phys. Rev. B56 (1997) 6620.
21. T. Nagao, J.T. Sadowski, M. Saito, S. Yaginuma, Y. Fujikawa, T. Kogure, T. Ohno, Y. Hasegawa, S. Hasegawa, and T. Sakurai, Phys. Rev. Lett. 93 (2004) 105501.
22. R. B. Campbell, J. M. Robertson, and J. Trotter, Acta Crystallogr. 14, 705(1961); R. B. Campbell and J. M. Robertson, Acta Crystallogr. 15 (1962) 289.
23. D. Holmes, S. Kumaraswamy, A. Matzeger, and K. P. C. Vollhardt, Chem. Eur. J. 5 (1999) 3399.
24. J. E. Northrup, Phys. Rev. B66 (2002)121404.
25. J. T. Sadowski, T. Nagao, S. Yaginuma, Y. Fujikawa, A. Al-Mahboob, K. Nakajima and T. Sakurai, (manuscript submitted to Appl. Phys. Lett.).
26. Akitaka Hoshino , Seiji Isoda, Hiroki Kurata, Takashi Kobayashi, J. Crys. Growth 146 (1995) 636.
27. W. Bollmann, Crystal defecst and Crystalline Interfaces, Berlin ; New York : Springer-Verlag (1970).
28. Mulliken, R. S., J. Chem. Phys. 23 (1955) 1833; Segall, M. D.; Pickard, C. J.; Shah, R.;
29. Payne, M. C., Mol. Phys. 89 (1996) 571; Segall, M. D.; Shah, R.; Pickard, C. J.; Payne, M. C., Phys. Rev. B54 (1996) 16317; Sanchez-Portal, D.; Artacho, E.; Soler, J. M. , Solid State Commun. 95 (1995) 685.
30. Hammer, B.; Hansen, L. B.; Norskov, J. K., Phys. Rev. B59 (1999) 7413.
31. WSxM© ; http://www.nanotec.es
32. Sadowski et al.(unpublished).

FIGURES

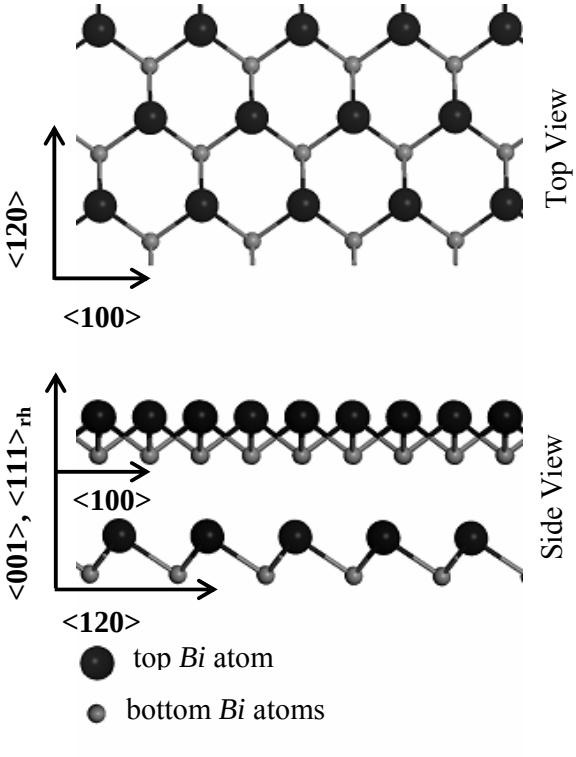

Fig.1 Top view and side view of cleaved (111) surface of the rhombohedral bulk Bi, having bilayer structure and hexagonal surface symmetry with no dangling bonds. The directions in hexagonal surface lattice are described without subscripts. The subscript 'rh' stands for rhombohedral system. The direction in rhombohedral system is the same as the cubic Si substrate used in our experiments.

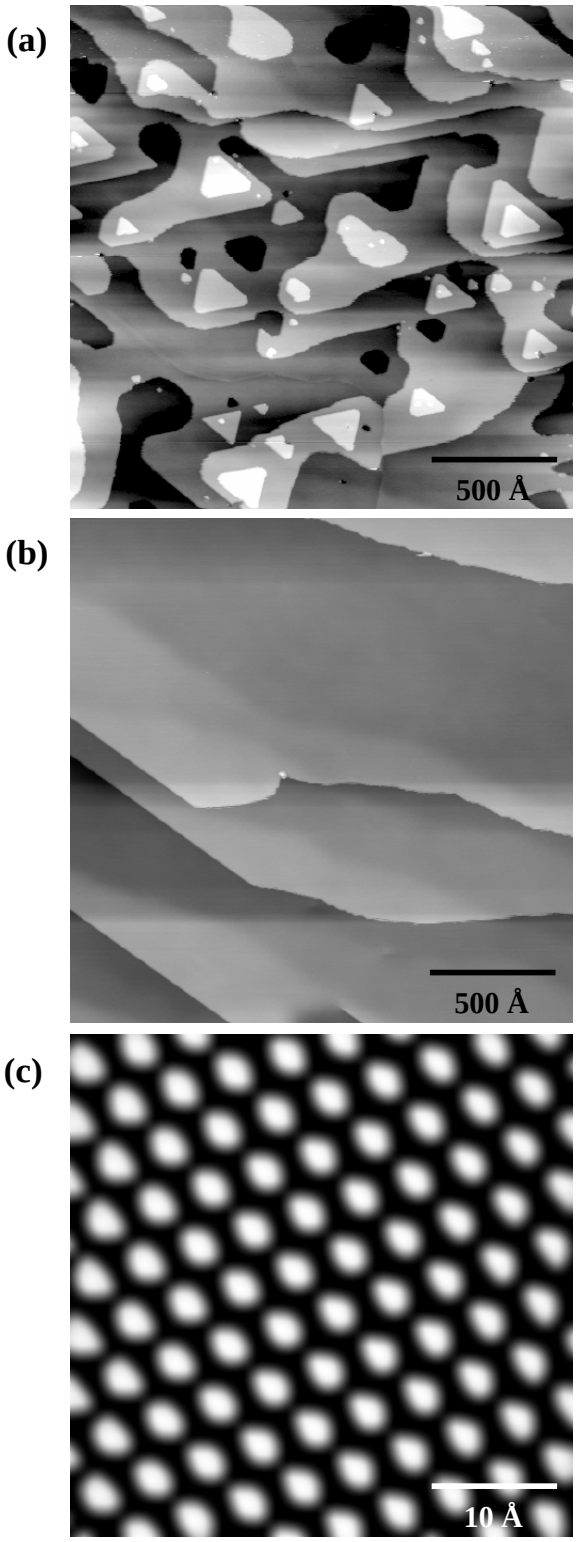

Fig.2 (a) Topographic, empty state STM image of the 21 BL_{001} thick Bi(001) film (sample bias +2.1 V, tunneling current 20 pA) taken right after RT Bi deposition on Si(111)-7x7; (b) Topographic STM image of the Bi film shown in (a) after annealing at ~ 410 K for 30 min. (sample bias +1.8 V, tunneling current 20 pA); (c) Atomic-resolution, empty state STM image (sample bias +0.04 V, tunneling current 300 pA) taken at the Bi(001) surface shown in (b).

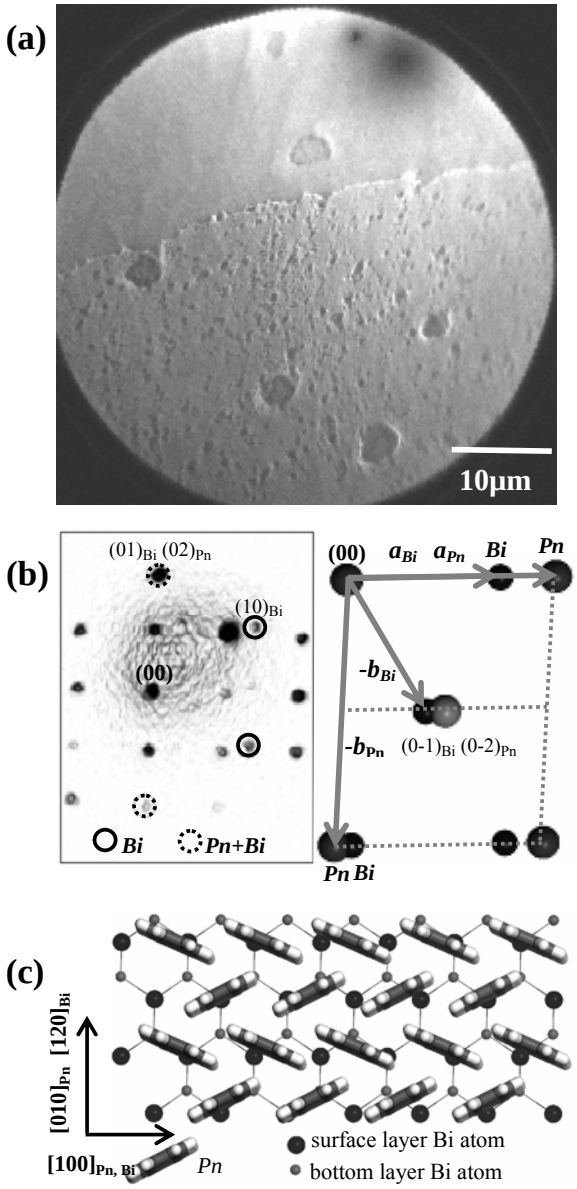

Fig.3 (a) LEEM image (E = 0.2 eV) showing Bi(001)/Si(111) surface partially covered by the first Pn layer (lower portion of the image); (b) LEED pattern (E = 16 eV) taken from the region shown in (a) – corresponding mapping into Pn molecular and Bi atomic positions is visualized at the right side, diffraction spots from both Pn layer and Bi(001) substrate are visible simultaneously; (c) Adsorption geometry (view form the direction normal to Pn(001) plane) for the first Pn layer adsorbed on Bi(001) surface, showing proposed commensurate "point-on-line" alignment with the Bi surface.

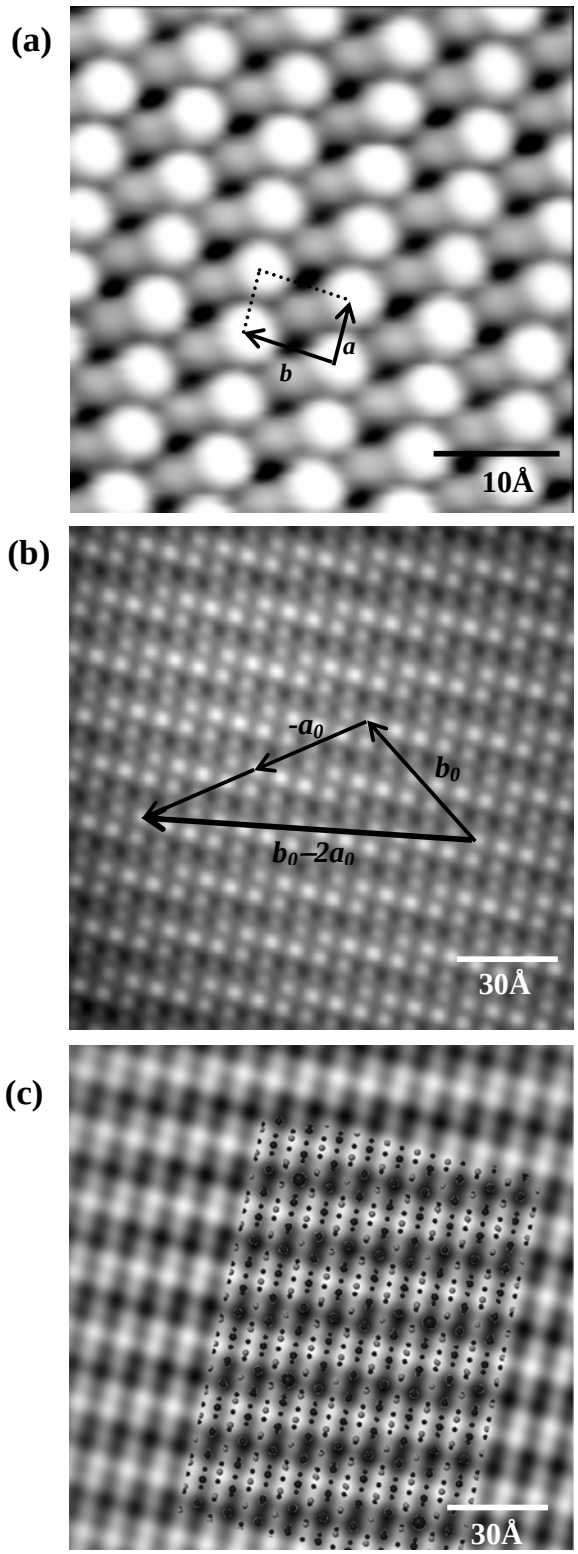

Fig.4 (a) Topographic, high-resolution, empty state STM image (sample bias +1.8 V, tunneling current 20 pA) of the first Pn layer; with each protrusion corresponding to the single Pn molecule – Pn unit cell in ab plane is outlined in the image; (b) Constant height, empty state STM image (sample bias +0.8 V, tunneling current 200 pA) of the pentacene monolayer completely covering the Bi(001) surface – the equivalent contrast positions are defined by vectors $-a_0$ and b_0, where $T= b_0-2a_0$ is the contrast modulation direction; (c) FFT filtered STM image shown in (b) with superimposed simulated geometry of oblique Pn and hexagonal Bi lattices at the interface.